

**Process Optimization of *Lycium ruthenicum* Murr.  
Powder Preparation by Airflow Ultrafine Pulverization at  
Low Temperature and Characterization of its Antioxidant Activity**

<sup>1,2,3</sup>Deng Kai, <sup>1,2</sup>Hu Na, <sup>1,2</sup>Suo Yourui and <sup>1,2</sup>Ding Chenxu\*

<sup>1</sup>Northwest Institute of Plateau Biology, Chinese Academy of Sciences,  
Key Laboratory of Tibetan Medicine Research, Xining, 810008.

<sup>2</sup>Northwest Institute of Plateau Biology, Chinese Academy of Sciences,  
Key Laboratory of Tibetan Medicine Research of Qinghai Province, Xining, 81008.

<sup>3</sup>University of the Chinese Academy of Sciences, Beijing, 100049.

cxding@nwipb.cas.cn\*

(Received on 1<sup>st</sup> January 2018, accepted in revised form 8<sup>th</sup> December 2018)

**Summary:** The processing of ultrafine pulverization *Lycium ruthenicum* Murr. by airflow is studied to determine the best parameters. Based on the single factor experiment, orthogonal experimental design is utilized to optimization of process parameters. The results show that the water content is 0.5%, air supply pressure is 0.70 Mpa, graded speed is 55 Hz, freezing time in the liquid nitrogen is 2 h. Under the condition of repeated trials, the average grading of *L. ruthenicum* fruit submicron powder is  $19.8167 \pm 0.53 \mu\text{m}$ . The contents of the total polysaccharides, anthocyanin and antioxidant activity in the water extract of submicron powders are obviously higher than the normal powder's, which can efficiently increase the dissolution rate of active ingredients in *L. ruthenicum* Murr.

**Key words:** Ultrafine pulverization by airflow; *Lycium ruthenicum* Murr; Technological parameter; Optimization; Low temperature.

## Introduction

*Lycium ruthenicum* Murr. belongs to perennial shrubs of the genus *Lycium* of the Solanaceae family and is widely distributed in the salinized deserts of northwest China. A unique medicinal and edible plant, it is mainly produced in China's Qinghai Province and Xinjiang Uygur Autonomous Region [1-2]. *L. ruthenicum* Murr., called "Para" in Tibetan medicine, has sweet flavor, mild nature, and can ameliorate heart heat. It is considered as a precious traditional Chinese herb in the Tibetan medical masterpiece called "shel gong shel phreng". *L. ruthenicum* Murr. can not only be eaten directly or consumed as a beverage, but it can also be used as a medicine for the treatment of heart disease, hypertension, irregular menstruation, climacteric disturbance, tinea and furuncle, urethral calculus, and gum bleeding [3]. Modern pharmacological studies have also shown that it has antioxidative, anti-atherosclerotic, pro-immunogenic, anti-hyperlipidemic, and anti-aging properties [4-8].

Ultrafine grinding technology is a new food processing method that was recently developed worldwide. Ultrafine grinding involves pulverizing a material into particles several micrometers in size by mechanical or hydrodynamic forces. The airflow

disintegrating mill, also called fluid energy mill, uses high pressure airflow to cause intense collision and friction among material particles and grind material particles by direct shearing [9-11].

## Experimental

### Materials and methods

### Materials and reagents

Fresh fruits of *Lycium ruthenicum* Murr. were purchased from Qinghai Danzhu Ming Qi Biological Development Technology Co. Ltd. All reagents used were of analytical grade. The total antioxidant capacity kits were purchased from the Nanjing Jiancheng Bioengineering Institute.

### Instruments and equipment

The TC-10 fluid-bed air flow crusher was produced by Langfang Xinlongli machinery manufacture company; the BT-9300LD laser particle size distribution instrument was purchased from Dandong Bettersize Instruments Co. Ltd.; the AL204 electronic balance was from Mettler Toledo Co. Ltd.

---

\*To whom all correspondence should be addressed.

The MB25 rapid moisture meter was from Shanghai Ouhaosi Instrument Co. Ltd.; the HH-2 electric-heated thermostatic water bath was produced by Beijing Kewei Yongxing Instrument Co. Ltd.; the 101 type electricity heat drum wind drying oven was from Beijing Ever Bright Medical Treatment Instrument Co. Ltd.; the FW135 herbal medicine grinding machine was produced by Tianjin Taisite Instrument Co. Ltd.; the KQ3200DE numerical control ultrasonic cleaner was from Kunshan Ultrasonic Instruments Co. Ltd.; the Epoch 2 ELIASA was from BioTek Instrument Co. Ltd.; the SU8000 cold field emission scanning microscope was produced by Hitachi (China) Co. Ltd.

#### Experimental methods

##### The technological process of fluid-bed airflow milling

The following is the process followed for fluid-bed airflow milling: Dried *L. ruthenicum* fruit → screening → drying → coarse milling → sieving → freezing → airflow ultrafine grinding → hierarchical collection → *L. ruthenicum* fruit ultrafine powder.

1. Screening removed the impurities from *L. ruthenicum* fruit.
2. Drying was performed to place pure *L. ruthenicum* fruit in an electrically-heated drum wind drying oven with controlled moisture.
3. Coarse milling was performed by coarse grinding of dried *L. ruthenicum* fruit using herbal medicine grinding machine to obtain particles that meet the requirements of airflow ultramicro pulverization.
4. Freezing was performed by putting *L. ruthenicum* dried fruit coarse powder into a liquid nitrogen container.
5. Airflow ultramicro pulverization was performed by placing *L. ruthenicum* fruit coarse powder in fluidized-bed airflow ultramicro pulverizer to achieve ultrafine powder of fruit after hierarchical collection.

##### Single factor experiment

1. Effect of graded speed on the particle size of *L. ruthenicum* fruit ultrafine powder. Under the same freezing time, moisture content, and air supply pressure, the effects of grading speed (35, 40, 45, 50 and 55 Hz) on the particle sizes of the ultrafine fruit powder were measured and analyzed.

2. Effect of freezing time on the particle size of ultrafine fruit powder. Under the same grading speed, water content, and air supply pressure, the effect of freezing time (0, 0.5, 1, 2, 4 h) on the particle sizes of ultrafine fruit powder was measured and analyzed.
3. Effect of water content on the particle size of ultrafine fruit powder. Under the same grading speed, freezing time, and air supply pressure, the effects of water content (0.5%, 2%, 4%, 6%, 8%) on the particle sizes of ultrafine fruit powder was measured and analyzed.
4. Effect of air supply pressure on the particle size of ultrafine fruit powder. Under the same grading speed, freezing time, and water content, the effects of air supply pressure (0.65, 0.70, 0.75, 0.80, 0.85 Mpa) on the particle size of ultrafine fruit powder was measured and analyzed.

##### Orthogonal optimization test

Based on the single factor test analysis and the principle of orthogonal test, the fruit powder cumulative particle size distribution rate of 90% of the particle size value ( $D_{90}$ ) was used as the response value to determine grading speed, freezing time, and water content, and each factor with three levels were analyzed using the  $L_9(3^3)$  orthogonal table. The results of the orthogonal optimization test are listed in Table-1.

Table-1: The factors and levels of orthogonal optimization design.

Levels	Factors		
	A (Grading speed/Hz)	B (Air supply pressure/Mpa)	C (Water content/%)
1	45	0.65	0.5%
2	50	0.70	2.0%
3	55	0.75	4.0%

##### Determination of powder size

The *L. ruthenicum* fruit ultrafine powder grinded by fluidized bed airflow ultramicro pulverizer was placed in a laser particle analyzer and its particle size was measured at room temperature.  $D_{90}$  was considered as the assessment standard.

##### Repeatability test

The optimized conditions achieved by orthogonal test were repeated thrice to measure the particle size.

*Component determination of ultrafine powder water extraction**Preparation of the water extract*

Pure water was added into a certain amount of *L. ruthenicum* fruit ultrafine powder or normal powder at the ratio of 1:25 at a temperature of 60°C, and ultrasonic extraction was performed for 25 min. The extraction was repeated thrice after suction filtration to achieve water extraction of the ultrafine powder and normal powder.

*Determination of total polysaccharides*

Drawing of the standard curve: 0.01 g glucose was precisely weighed after drying at 105°C, placed in a volumetric flask, dissolved in water, and diluted to the scale. The glucose standard solution was prepared after shaking. Precisely 0.1, 0.2, 0.4, 0.6, 0.8, 1.0 mL glucose standard solution was taken in 10 mL volumetric flasks, followed by rapid addition of 2.0 mL distilled water, 1.0 mL 5% phenol solution, and 5.0 mL concentrated sulfuric acid with shaking. Then, the mixture was placed in a 40°C water bath for 15 min and put into cold water for 10 min. At the same time, 2.0 mL distilled water was taken as the blank sample. The absorbance was detected using a microplate reader at a wavelength of 490 nm. The obtained standard curve equation was  $A = 36.897C + 0.1072$  with a correlation coefficient  $r = 0.9999$ , where C was the concentration of glucose and A was the absorbance.

The polysaccharide content and extraction yield were determined by phenol-sulfuric acid method. Precisely, 1 mL of the sample solution was taken, placed in a 25 mL volumetric flask, and diluted with water to constant volume. Then, 1 mL of the diluted solution was placed in a 10 mL volumetric flask, followed by addition of 2 mL water and 1.0 mL 5% phenol solution. After shaking, 5.0 mL concentrated sulfuric acid was rapidly added and the mixture was placed in a 40°C water bath for 15 min, followed by incubation in cold water for 10 min. At the same time, 2.0 mL distilled water was used as the blank. The absorbance was detected using a microplate reader at a wavelength of 490 nm absorbance[12]. The extraction yield of polysaccharides was calculated using the following formula:

$$\text{The total polysaccharide content \%} = C \cdot D \cdot F / W \times 100\% \quad (1)$$

where, C is the concentration of glucose standard solution; D is the dilution factor; F is conversion value; W is the sample quality.

*Determination of anthocyanin content*

The maximum absorbance wavelengths and the maximum absorbance  $A_{\lambda_{\max}}$  of anthocyanin in aqueous solution of *L. ruthenicum* fruit ultrafine powder and normal powder were measured using a microplate reader in the range of 250 to 600 nm with pH 4.5 and pH 1.0 buffer[13]. The total anthocyanin content was calculated using the following formula (calculated as cyanidin-3-glucoside):

$$A = A_{\lambda_{\max} \text{ pH } 1.0} - A_{\lambda_{\max} \text{ pH } 4.5}$$

$$C = (A \times 103 \times MW \times DF) / (\epsilon \times l)$$

$$\text{The total anthocyanin content (mg/100g)} = (C \times V) / M \times 10 \quad (2)$$

where,  $A_{\lambda_{\max}}$ : the maximum absorbance at the maximum absorbance wavelengths; MW: the molecular weight of cyanidin 3-glucoside (449.2 g/mol); DF: dilution factor of the testing solution;  $\epsilon$ : extinction coefficient (29600 L/mol-cm); l: optical path length (cm); C: anthocyanin mass concentration (mg/L); V: volume of testing solution (mL); M: sample weight (g).

*ABTS free radical scavenging assay*

ABTS can be oxidized into green  $ABTS^+$  using a proper oxidant, whereas  $ABTS^+$  generation was inhibited in the presence of an antioxidant. Thus, the absorbance of  $ABTS^+$  at 405 nm or 734 nm can be detected to calculate the total antioxidant capacity of samples. Trolox, an analogue of VE with similar antioxidant capacity, was used as a reference for determining the total antioxidant capacity of other antioxidants[14].

Trolox standard solution (10 mM) was diluted to 0.1, 0.2, 0.4, 0.8, and 1.0 mM with double distilled water. Ten microliters diluted solution was added into each well and 10  $\mu$ L double distilled water was used as the control. Then, 20  $\mu$ L reagent four and 170  $\mu$ L ABTS solution were added to each well and reacted for 6 min at room temperature. The OD values were detected at 405 nm to obtain the ABTS standard curve with the equation  $A = -0.7373C + 1.0832$ ,  $R^2 = 0.9998$ , where A was the absorbance value and C was the concentration of Trolox standard

solution. When the inhibition rate of the solution was the same as that of a certain molar concentration of Trolox, the calculation was performed by dividing the mass of extracts with the molar concentration of Trolox, and the result was expressed as mM/g.

#### FRAP free radical scavenging assay

The ferric reducing power of plant extracts was determined using a modified version of the FRAP assay. This method is based on the reduction, at low pH, of a colorless ferric complex ( $\text{Fe}^{3+}$ -tripirydyltriazine) to a blue-colored ferrous complex ( $\text{Fe}^{2+}$ -tripirydyltriazine) by the action of electron-donating antioxidants. The reduction is monitored by measuring the change of absorbance at 593 nm. The working FRAP reagent was prepared daily by mixing 10 volumes of 300 mM acetate buffer, pH 3.6, with 1 volume of 10 mM TPTZ (2,4,6-tri(2-pyridyl)-s-triazine) in 40 mM hydrochloric acid and with 1 volume of 20 mM ferric chloride. A standard curve was prepared using various concentrations of  $\text{FeSO}_4 \cdot 7\text{H}_2\text{O}$ . All solutions were used on the day of preparation. 100  $\mu\text{L}$  of sample solutions and 300  $\mu\text{L}$  of deionized water were added to 3 mL of freshly prepared FRAP reagent. The reaction mixture was incubated for 30 min at 37 °C in a water bath. Then, the absorbance of the samples was measured at 593 nm. A sample blank reading using acetate buffer was also taken. The difference between sample absorbance and blank absorbance was calculated and used to calculate the FRAP value. In this assay, the reducing capacity of the plant extracts tested was calculated with reference to the reaction signal given by a  $\text{Fe}^{2+}$  solution. FRAP values were expressed as  $\text{mmol Fe}^{2+}/\text{g}$  of sample [15]. All measurements were done in triplicate.

#### Scanning electron microscopy (SEM)

A certain amount of *L. ruthenicum* fruit powder was dried to constant weight and the surface was gold-plated by ion sputtering. The gold-plated sample was placed on the objective table. Then, a high voltage was applied to observe the morphology of the sample under low magnification. After selection of the visual field, the particle structure and morphology were observed at 400  $\times$  magnification.

#### Statistical Analysis

Data were shown as means  $\pm$  S.D. from three independent experiments. Statistical analysis

was performed by one way ANOVA or student's t-test using the statistical analysis software SPSS 18.0.  $P < 0.05$  was considered statistically significant.

#### Results and analysis

##### Analysis of single factor testing

##### Effects of grading speed on the particle size of *Lycium ruthenicum* Murr. fruit ultrafine powder

As shown in Fig. 1, under the same freezing time, water content, and air supply pressure, increase in grading speed gradually decreased  $D_{90}$  of the *L. ruthenicum* fruit ultrafine powder. This is because the high-speed revolution of the grader impeller generated large amounts of centrifugal force, and when rotated in the impeller, the *L. ruthenicum* fruit experienced centrifugal force and dielectric resistance in a direction opposite to that of the centrifugal force. When the centrifugal force was larger than the resistance, the particle flew to the grinding room to be crushed by the airflow. The particle passed through the grader impeller and entered the collection system with the airflow when the centrifugal force was smaller than resistance. The rotational speed of the grader impeller increased with sorting frequency. The particle size decreased with ideal grinding effectiveness when the centrifugal velocity increased.  $D_{90}$  was 47.5  $\mu\text{m}$  when the grading speed was 35 Hz, whereas  $D_{90}$  was 27.02  $\mu\text{m}$  when grade speed was 55 Hz. Therefore, during horizontal screening, the speed range of the pulverizer was set at 0-55 Hz, and 45-55 Hz was selected as the horizontal numerical value optimized by the orthogonal experimental process.

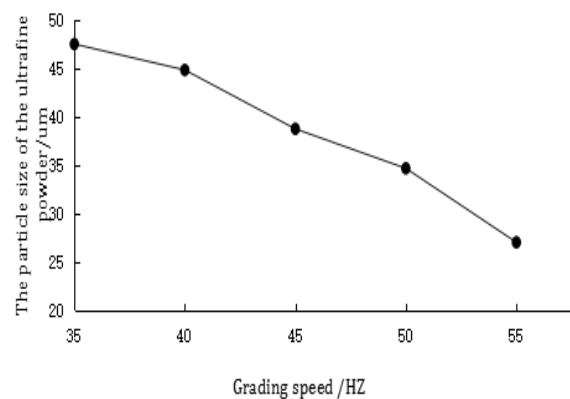


Fig. 1: Effects of grading speed on the particle size of *Lycium ruthenicum* Murr. fruit ultrafine powder

### Effect of freezing time on the particle size of *L. ruthenicum* fruit ultrafine powder

As shown in Fig. 2, under the same grading speed, water content, and air supply pressure,  $D_{90}$  of *L. ruthenicum* fruit ultrafine powder significantly decreased with the increase in the freezing time in liquid nitrogen. Compared to 0 h freezing,  $D_{90}$  at 0.5 h freezing time reduced from 24.74  $\mu\text{m}$  to 21.33  $\mu\text{m}$ . This is because after freezing in liquid nitrogen, the water molecules in *L. ruthenicum* fruit coarse powder formed ice crystals, which reduced intermolecular forces; thus, the material became fragile and was easily crushed. In contrast, when the freezing time was increased to 2-4 h,  $D_{90}$  changed from 17.4  $\mu\text{m}$  to 16.78  $\mu\text{m}$  and the changes in particle size were negligible; this could be because optimum intermolecular forces and degree of water crystallization were achieved within 2 h of freezing, and therefore, prolongation of freezing time showed no significant effects. Hence, 2 h was chosen as the optimum freezing time for the actual production.

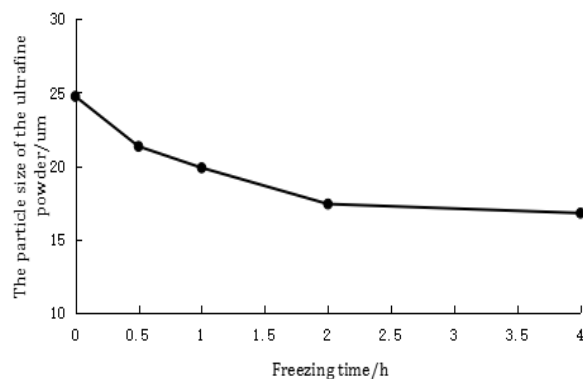


Fig. 2: Effect of freezing time on the particle size of *L. ruthenicum* fruit ultrafine powder

### Effects of water content on the particle size of *L. ruthenicum* fruit ultrafine powder

As shown in Fig. 3, under the same grading speed, freezing time, and air supply pressure,  $D_{90}$  of *L. ruthenicum* fruit ultrafine powder slightly increased with increase in water content.  $D_{90}$  was 28.69  $\mu\text{m}$  when the water content was 0.5%, whereas  $D_{90}$  was 34.53  $\mu\text{m}$  when the water content was 4%.  $D_{90}$  increased rapidly when the water content was higher than 4%.  $D_{90}$  was 59.5  $\mu\text{m}$  when the water content was 8%. This is

because high water content increased the humidity of *L. ruthenicum* fruit powder and caused adhesion and accumulation of the ultrafine powder and water on the inner walls of the grader impeller upon collision with high-speed airflow. This situation could increase the sorting resistance of the grader, resulting in an increase in the water content as well as particle size. Hence, the water content should be below 4% during ultrafine grinding. Water content higher than 4% during the experiment will affect the grader efficiency, leading to coherence during production, and show no benefit in the collection and storage of powders. Therefore, 0.5-4% water content was chosen as the optimal value after the orthogonal test.

### Effects of air supply pressure on the particle size of *L. ruthenicum* fruit ultrafine powder

According to Fig. 4, under the same freezing time, grading speed, and water content,  $D_{90}$  of *L. ruthenicum* fruit ultrafine powder decreased with increase in air supply pressure. This is because the kinetic energy of airflow formed by high-speed electromagnetic valve increased with increase in air supply pressure, and the airflow caused rapid collision of material particles leading to finer particle size of *L. ruthenicum* fruit ultrafine powder. However, when the air supply pressure reached 0.7 Mpa, the particles show a minimum size of 30.3  $\mu\text{m}$ . Particle size increase was not observed with increase in air supply pressure. This might be because the *L. ruthenicum* fruit powder contains more sugar and is prone to form small particles under high-speed airflow, which might increase the resistance of impeller and increase the particle size of the ultrafine powder after grading. Hence, 0.65-0.75 Mpa air supply pressure was selected after the orthogonal test.

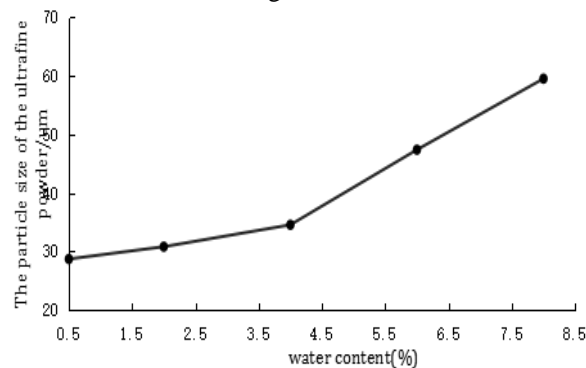


Fig. 3: Effects of water content on the particle size of *L. ruthenicum* fruit ultrafine powder

## Results and analysis of orthogonal test

Based on single factor analysis and orthogonal optimization test principles,  $D_{90}$  was used as the response value for designing grading speed, freezing time, and water content, and each factor with three levels was analyzed using the  $L_9(3^3)$  orthogonal table. The results of orthogonal optimization test were processed and analyzed using the SPSS software.

The three factors, namely, grading speed, air supply pressure, and water content were used for the  $L_9(3^3)$  orthogonal test and the results are shown in Table-3. According to Table-3, the P values of A, B, and C were lower than 0.005, indicating the significant influence of these three factors on particle size. The SD analysis suggested the strongest factor that affected the low-temperature ultrafine grinding of *L. ruthenicum* fruit was A, followed by C and B. In other words, the factors in the order of influence were grading speed, water content, and air supply pressure. As shown in Table-4, 5, and 6, the optimum extraction condition for low temperature ultrafine crushing was A1B2C1, which indicates that the optimum conditions were 2 h of freezing time with 55 Hz grading speed, 0.5% water content, and 0.7 Mpa air supply pressure.

Table-2: Orthogonal optimization design.

Numbers	Grading speed /Hz	Air supply pressure /Mpa	Water content /%	Particle size/ $\mu\text{m}$
1	1	1	1	37.31
2	1	2	2	36.98
3	1	3	3	38.20
4	2	1	3	32.78
5	2	2	1	30.62
6	2	3	2	31.45
7	3	1	2	22.56
8	3	2	3	22.90
9	3	3	1	21.74

Table-3: Orthogonal test result analysis.

Dependent variable: Particle size					
Source	Type III sum of Squares	df	Mean Square	F	P
Corrected Model	351.300 <sup>a</sup>	6	58.550	8901.174	.000
Intercept	8374.690	1	8374.690	1273179.250	.000
A (Grading speed)	347.431	2	173.715	26409.427	.000
B (Air supply pressure)	.778	2	.389	59.140	.017
C (Water content)	3.091	2	1.545	234.954	.004
Error	.013	2	.007		
Total	8726.003	9			
Corrected Total	351.313	8			

Table-4: The affection of grading speed to the particle size.

Grading speed	N	Subset		
		1	2	3
55Hz	3	22.4000		
50Hz	3		31.6167	
45Hz	3			37.4967
P		1.000	1.000	1.000

Table-5: The affection of air supply pressure to the particle size.

Air supply pressure	N	Subset		
		1	2	3
0.70Mpa	3	30.1667		
0.75Mpa	3		30.4633	
0.65Mpa	3			30.8833
P		1.000	1.000	1.000

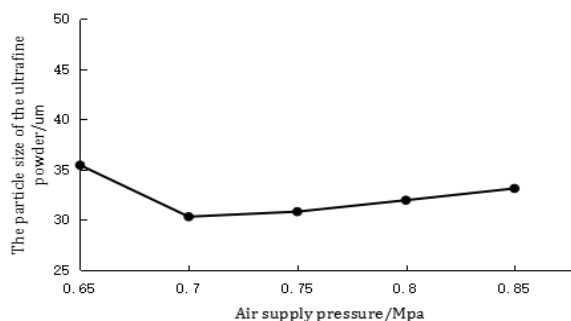
Table-6: The affection of water content to the particle size.

Water content	N	Subset		
		1	2	3
0.5%	3	29.8900		
2%	3		30.3300	
4%	3			31.2933
P		1.000	1.000	1.000

The same batch of *L. ruthenicum* fruit coarse powder was ultrafine grinded following the methods described in 1.3.1. The experiments were performed thrice with grading speed as 55 Hz, 0.7 Mpa air supply pressure, and 0.5 % water content. The obtained *L. ruthenicum* fruit ultrafine powder have a homogeneous size of  $19.8167 \pm 0.53 \mu\text{m}$  and  $\text{RSD} = 2.6979\%$ , indicating good repeatability of this method.

Determination of the contents of total polysaccharide and anthocyanin of *L. ruthenicum* fruit powder

As shown in Fig. 5, the total polysaccharide content of an aqueous solution of the ultrafine powder ( $42.68 \pm 0.11\%$ ) was significantly higher than that of the normal powder ( $34.52 \pm 0.13\%$ ). The reason was that *L. ruthenicum* fruit contains polysaccharides, proteins, and vitamins, and after ultrafine grinding, the water base of *L. ruthenicum* fruit was exposed to increased water binding capacity. Thus, under the same extraction conditions, cells in *L. ruthenicum* fruit powder were crushed and the polysaccharides in the ultrafine powder dissolved easily in water under the effects of pressure, friction, and shearing force, resulting in higher extraction efficiency.

Fig. 4: Effects of air supply pressure on the particle size of *L. ruthenicum* fruit ultrafine powder.

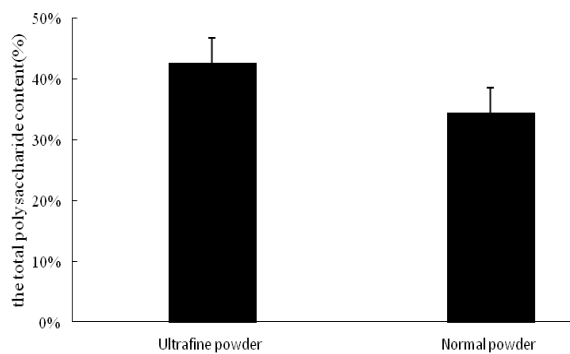


Fig. 5: Determination of the total polysaccharide content.

Fig. 6 shows that under the same ultrasonic-assisted extraction conditions, the anthocyanin content of an aqueous solution of the ultrafine powder was remarkably improved compared to that of the normal powder. The anthocyanin contents of ultrafine powder and normal powder were  $74.71 \pm 2.8$  mg CGE/g and  $49.54 \pm 1.99$  mg CGE/g, respectively. The changes in anthocyanin content indicated that the destruction of tissue structure and cell wall after ultrafine grinding could promote dissolution of anthocyanin.

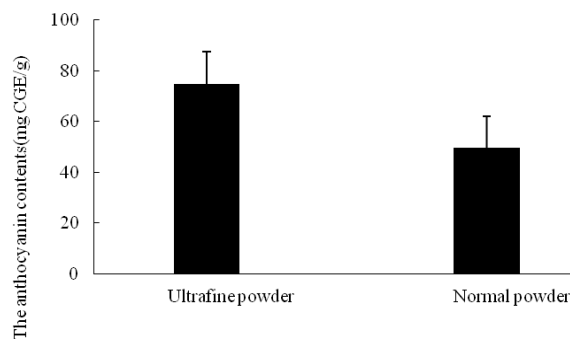


Fig. 6: Determination of anthocyanin content

#### ABTS radical scavenging capacity of *L. ruthenicum* fruit powder

As shown Fig. 7, the total antioxidant capacity of an aqueous solution of *L. ruthenicum* fruit ultrafine powder and normal powder were analyzed using the ABTS methods. We observed that under the same extraction conditions, the total antioxidant capacity of the ultrafine powder ( $0.916 \pm 0.03$  mM/g) was significantly higher than that of normal coarse

powder ( $0.726 \pm 0.04$  mM/g). Therefore, the ultrafine powder could efficiently increase the dissolution of antioxidant components in *L. ruthenicum* fruit.

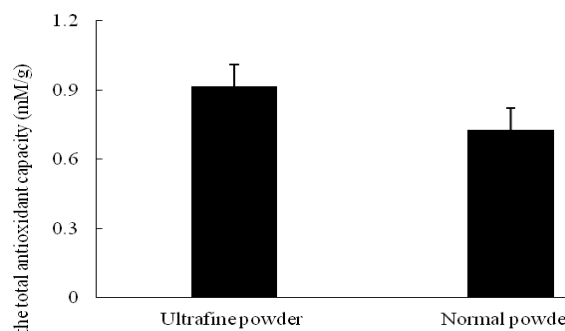


Fig. 7: The total antioxidant capacity by ABTS.

#### FRAP radical scavenging capacity of *L. ruthenicum* fruit powder

As shown in Fig. 8, the total antioxidant capacity of an aqueous solution of *L. ruthenicum* fruit ultrafine powder and normal powder were analyzed using the FRAP method. We observed that under the same extraction conditions, the total antioxidant capacity of the ultrafine powder ( $1.5237 \pm 0.004$  mmol  $\text{Fe}^{2+}$ /g) was considerably higher than that of the coarse powder ( $1.2243 \pm 0.006$  mmol  $\text{Fe}^{2+}$ /g). Therefore, ultrafine grinding could efficiently destroy cell walls to improve the dissolution of antioxidant components in *L. ruthenicum* fruit.

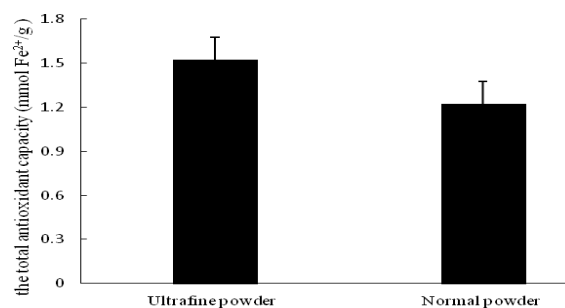
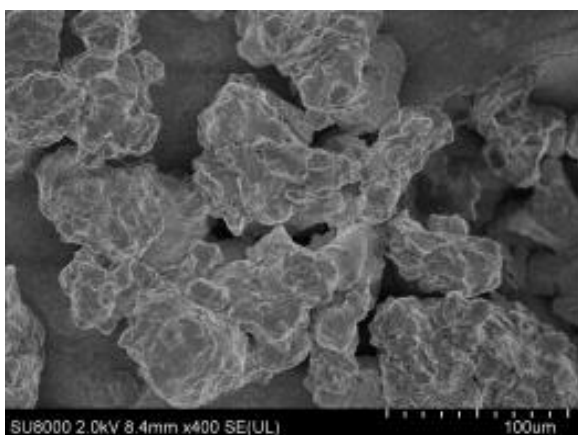
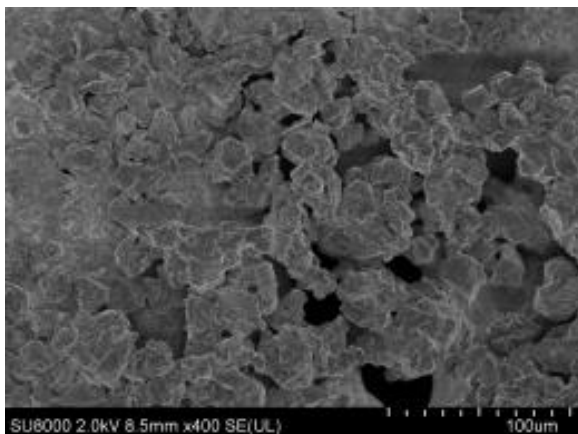


Fig. 8: The Total antioxidant capacity by FRAP.

#### Scanning electron microscopy (SEM) of *L. ruthenicum* fruit powder

The ultrafine and normal powders of *L. ruthenicum* fruit were observed by SEM as shown in Fig. 9 ( $\times 400$ ). The normal powder of *L. ruthenicum* fruit showed larger particle size with clear connection

between tissues, irregular shape, and uneven particle size. After ultrafine grinding, the particle size of the ultrafine powder of *L. ruthenicum* fruit decreased significantly and no obvious large particles with less connections among tissues, homogeneous particle size, and regular shape were detected. The tissue structures were partially destroyed.



(a) Ultrafine fruit powder and (b) Normal fruit powder of *Lycium ruthenicum* Murr.

Fig. 9: SEM images of *Lycium ruthenicum* Murr. fruit powder ( $\times 400$ ).

### Conclusions

*L. ruthenicum* fruit was used as the raw material for airflow ultrafine grinding. According to the single factor analysis and orthogonal optimization test principles, as well as the practical situation, the optimum grinding process parameters were 0.5% water content, 0.70 MPa air supply pressure, and 55 Hz grading speed. The experiment was repeated under the optimum conditions and the mean particle

size of *L. ruthenicum* fruit ultrafine powder obtained was  $19.8167 \pm 0.53 \mu\text{m}$ . Thus, the established model in this experiment could better represent the process conditions of airflow ultrafine grinding. The particle size of *L. ruthenicum* fruit powder treated by airflow ultrafine grinding was  $19.8167 \pm 0.53 \mu\text{m}$ , which was lesser than  $20 \mu\text{m}$ . Additionally, the polysaccharide content, anthocyanin content, and antioxidant capacity of the ultrafine powder in aqueous solution was significantly higher than those of the normal powder. The SEM images indicated that airflow ultrafine grinding could effectively destroy the tissue structure and decrease particle size.

The extent of *L. ruthenicum* fruit-based product development is low since most products are currently utilized as primary commodity. Since *L. ruthenicum* fruit usually enters the market as original food or raw material, its added value and utilization are low. Hence, the economic benefit of resource exploitation and utilization is not remarkable, which inhibits the development of such bioresources. Airflow ultrafine grinding-treated *L. ruthenicum* fruit improves assimilation of bioactive substances in the human body in the form of small molecules in different physical states, which is a promising development for biological resources such as berries.

### Acknowledgements

This study was supported by Science and Technology Support Plan in Qinghai Province (2015-SF-123), Development and Construction of key Laboratories in Qinghai Province (2017-ZJ-Y11).

### References

1. H. H. Zhang, X. li, J. G. Wang, The Structure Characteristic of the Plant Community in the Lower Reaches of Tarim River. *Ecol.Environ.*, **16**, 1219 (2007).
2. J. Zheng, C. Ding, L. Wang. Anthocyanins composition and antioxidant activity of wild *Lycium ruthenicum* Murr. from Qinghai-Tibet Plateau. *Food.Chem.*, **126**, 859 (2011)
3. Y. M. Liu., *Pharmacography of Uighur*, 253 (1999).
4. N. Hu,J. Zheng,W. Li., Isolation, stability, and antioxidant activity of anthocyanins from *Lycium ruthenicum* Murray and *Nitraria Tangutorum* Bobr of Qinghai-Tibetan plateau. *Sep.Sci.Technol.*, **49**, 2897 (2014)
5. Z. Liu, J. Dang, Q. Wang. Optimization of polysaccharides from *Lycium ruthenicum* fruit



- using RSM and its anti-oxidant activity. *Int.J.Biol.Macromol.*, **61**, 134 (2013).
6. L. Lin, J. Li, H. Y. Li, Effect of Lycium ruthenicum anthocyanins on atherosclerosis in mice. *China.J.Chin.Mater.Med.*, **10**, 1460 (2012).
  7. Q. Z. Jia, D. Y. Tao, Y. Chen. Activation of *Lycium Ruthenicum* Murr. Pigment on mice macrophage. *J.Tradit.Chin.Vet.Med.*, **27**,29(2008).
  8. D. Y. Tao, J. J. Chen, Y. Chen. Research in the anti-senile Function of *Lycium Ruthenicum* Murr. Pigment in Mice. *China.J.Chin.Mater.Med.*,**27**, 11 (2008).
  9. M Zhang, C Zhang, S Shrestha. Study on the preparation technology of superfine ground powder of *Agrocybe chaxingu* Huang, *J.Food. Eng.*, **67**, 333 (2005)
  10. J Hu, Y Chen, D Ni. Effect of superfine grinding on quality and antioxidant property of fine green tea powders, *LWT-Food.Sci.Technol.*, **45**,8( 2012)
  11. X. Y. Zhao, F. L. Du and Q. J. Zhu. Effect of Superfine Pulverization on Properties of Astragalus Membranaceus Powder, *Powder. Technol.*, **203**, 620 (2010).
  12. T Masuko, A Minami, N Iwasaki, T Majima, S. I. Nishimura, and Y. C. Lee. Carbohydrate analysis by a phenol-sulfuric acid method in microplate format. *Anal.Biochem.*, **339**,69, (2005)
  13. J Lee, R.W. Durst, R.E. Wrolstad. Determination of total monomeric anthocyanin pigment content of fruit juices, beverages, natural colorants, and wines by the pH differential method: collaborative study. *JAOAC.Int.*, **88**,1269 (2005)
  14. R Re, N Pellegrini, A Proteggente, A Pannala, M Yang, and C Rice-Evans. Antioxidant activity applying an improved ABTS radical cation decolorization assay. *Free.Radical.Bio.Med.*, **26**, 1231 (1999)
  15. K Thaipong,U Boonprakob, K Crosby, L Cisneros-Zevallos, and D. H. Byrne. Comparison of ABTS, DPPH, FRAP, and ORAC assays for estimating antioxidant activity from guava fruit extracts. *J.Food.Compos.Anal.*,**19**, 669 (2006).